IDENTIFICATION OF INTRINSIC CARBON FIBRES OXIDATION KINETICS FROM EXPERIMENTAL DATA AND CFD MODELING

N. Bertrand*, J. Lachaud, G. Bourget, F. Rebillat and G.L. Vignoles

Laboratoire des Composites Thermostructuraux
UMR 5801 (CNRS-Safran-CEA-University of Bordeaux 1)
3 Allée de la Boétie
33600 Pessac, France
*(corresponding author : bertrand@lcts.u-bordeaux1.fr)

ABSTRACT

The oxidation kinetics of carbon fibres are determined by measurement of mass loss in a cylindrical oxidation reactor. In order to identify reactional and diffusional regimes, and to provide a safe method for the identification of the intrinsic heterogeneous reaction rate, a CFD-based approach has been developed.
In this work, diffusion of the oxidant is considered throughout the reactor (global-scale modeling) and between individual fibres (local-scale modeling), in combination with convection and reactions. Homogeneous reactions of carbon and oxygen are considered according to thermodynamical data. The experimental heterogeneous reaction flux is entered in the model, and Péclet, Damköhler and Thiele dimensionless numbers are evaluated. These are measures of the importance of the reaction rate relatively to convection, global-scale and local-scale diffusion, respectively. When all numbers are low enough, it is possible to ensure that the acquired mass loss data are significant with respect to heterogeneous reaction ; when these numbers are higher, it is still possible to extract from the experimental data corrected values of the intrinsic reaction rates.

1. INTRODUCTION

Carbon-carbon (C-C) composites are commonly used materials for high temperature applications (up to 2500 °C) in corrosive environments (*e.g.* rocket nozzles, reentry tips, brake discs in aeronautic and space industry) [1]. Under these extremely severe conditions, a limited oxidation of these composites is unavoidable. Lifetime of C-C composites is assumed to depend on the oxidation resistance of fibres on one side, and of matrix on the other side. This work proposes two interdependent approaches in order to provide a safe method for the identification of heterogeneous reaction rate. It consists first in the measurements of mass loss of carbon fibres bundle in a cylindrical reactor. Then, transfer phenomena in this reactor are simulated using a CFD 3D-approach, allowing a rigorous identification of the intrinsic oxidation rate of carbon fibres.

2. EXPERIMENTAL

2.1. Context

Thermogravimetric analyses are currently used in order to evaluate the behaviour of fibres with respect to oxidation and to propose global kinetic laws [2]. Arrhenius plots of the experimental rates show a neat discontinuity, with a slope change around 620°C. Two main phenomena could explain this discontinuity.

(i) Thermochemical data (figure 1) indicate a change in the heterogeneous kinetic mecanism of oxidation of carbon around 700°C.

T < 700°C :

$C_{(s)} + O_{2\,(g)} \rightleftarrows CO_{2\,(g)}$ (1)

T > 700°C :

$2C_{(s)} + O_{2\,(g)} \rightleftarrows 2CO_{(g)}$ (2)

$2CO_{(g)} + O_{2\,(g)} \rightleftarrows 2CO_{2\,(g)}$ (3)

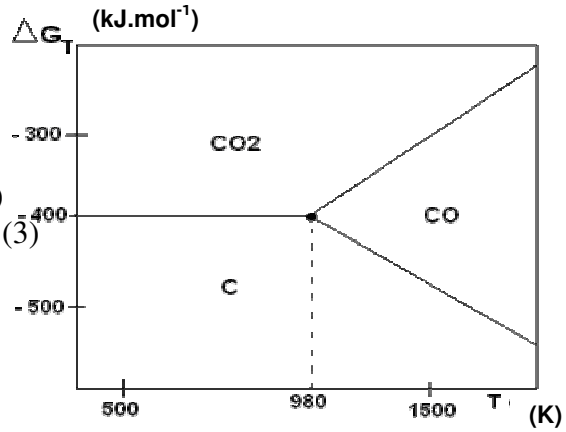

Figure 1: *Thermochemical data and heterogeneous reactions of carbon and oxygen* [3]

(ii) Considering heterogeneous reactions, mass transfer by diffusion and by reaction are coupled and in competition. For low temperatures, mass transfer phenomena are limited by reaction : this is the reactive (or reaction-limited) regime. At higher temperatures, mass transfer by reaction is faster and mass transfer by diffusion becomes limiting : this is the diffusional (or diffusion-limited) regime.

This work aims to identify these regimes and explain the discontinuity in the oxidation data.

2.1. Oxidation reactor and data

Repeatable experiments have been carried out in a cylindrical oxidation reactor at a controlled temperature (625 °C) under dry air at atmospheric pressure. The reactor section is a 14 mm diameter half-disk. Its effective length is 30 cm. The sample is reduced to a 1 cm^2 square surface incorporated in the center of the lower wall of the reactor (figure 2). The average velocity of the flow is 1 $m.s^{-1}$. This value has been chosen to ensure a high laminar oxygen injection flow. The materials tested are carbon fibres disposed as a bundle. The fibre bundle is made of approximately 600,000 cylindrical fibres in a non-compact array. Indeed,

it is practically impossible to arrange these fibres in a compact array. As discussed later, it will be necessary to take into account the local porosity of the bundle.

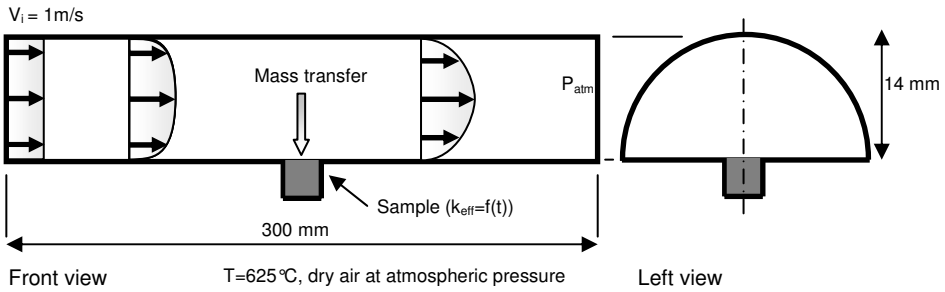

Figure 2: *Oxidation reactor geometry and experimental conditions (dry air at 625°C and 1 atm)*

The oxidation of ex-PAN, ex-pitch and ex-cellulose fibres under the experimental conditions described above is studied by measuring the mass loss versus time. These carbon fibres have been chosen because their different reactivity with respect to oxidation allows to explore a large interval of kinetic rate values.
The references used for these fibres and their characteristics are the following:

Fibre reference	**Material**	**Treatment at 1673K**	**Graphitization**
F1	ex-cellulose	√	
F2	ex-cellulose		
F3	ex-pitch	√	
F4	ex-pitch		
F5	ex-PAN (T300)	√	√
F6	ex-PAN (T300)	√	
F8	ex-PAN (M40)		
F9	ex-PAN (T300) (fibres bundle)		
F10	ex-PAN (M40)	√	

Table 1: *Fibres studied: references and characteristics*

The raw experimental data is the effective mass flow consumption of carbon per unit surface and time (J_{eff} in $g(C).m^{-2}.s^{-1}$). Then, the CFD study gives a correlation between J_{eff} and the effective reactivity of the carbon fibres bundle (k_{eff} in $m.s^{-1}$).

3. MODELLING AND ANALYSIS

3.1. Global-scale analysis

At a global scale, it is important to ensure that there is no limitation imposed by the process parameters. In order to evaluate the limiting transfer phenomena, a dimensionless approach is proposed. The Péclet mass number is first calculated in order to compare convection and mass diffusion velocities. If Pé = $v\delta_{diff}/D$ is lower than 1, where D is the gas diffusion coefficient and δ_{diff} is the diffusive boundary layer thickness, mass transfer is limited by convection. If Pé is larger than 1, global diffusional phenomena become limiting. In the present case, the boundary layer could not reach the reactor diameter. The Damköhler number Da = $k\delta_{diff}/D$ gives a comparison between mass diffusion and reaction velocities. When Da is lower than 1, mass transfer in the bulk fluid phase is limiting. Finally, high Pé and low Da numbers ensure that the oxidation phenomena are globally controlled by reaction mass transfer in the bulk fluid phase.

3.2. Local-scale analysis

The global study is not sufficient to evaluate the mass transfer phenomena at a local scale. The real oxidation rate of the fibres k_f can be derived from k_{eff}, the effective reaction rate of a fibre bundle, which is the experimentally accessible quantity as explained above.

Carbon fibres are assumed homogeneous and isotropic. The chemical reactions are restricted to the fibre surface. At 898 K in dry air at atmospheric pressure, the heterogeneous chemical reaction is considered first-order (see eq. [1]). The local impinging flux per surface unit is given by $J_y(x) = k_f C(x)$, with C(x) (in $mol.m^{-3}$) the oxygen concentration at position x (figure 3). Thermal gradients induced by reaction enthalpy are negligible [4].

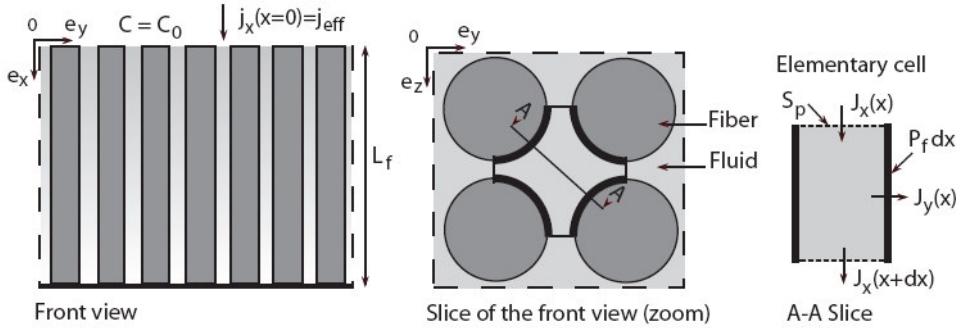

Figure 3: *Sketch of a unidirectional bundle of cylindrical fibres*

It is assumed that the local porosity of the bundle is homogeneous and the tortuosity is negligible along $\mathbf{e_x}$ axis.
Mass loss is strongly coupled to mass transfer between the fluid phase and the wall. The diffusion regime inside the porous media is given by the Knudsen number (Kn = $\overline{\lambda}/\overline{d_p}$, where $\overline{\lambda}$ is the mean free path and $\overline{d_p}$ is the mean pore length in the ($\mathbf{e_y}$, $\mathbf{e_z}$) planes). For a porous medium of

porosity ε and surface area S the mean pore diameter is approximated by [5]:

$$\overline{d_p} = \frac{4\varepsilon}{S} \tag{4}$$

For this case, assuming cylindrical fibres, one derives :

$$\overline{d_p} = \frac{4\overline{S_p}}{\overline{P_f}} = \overline{d_f}\left(\nu_c \mu_f / m_f - 1\right) \tag{5}$$

where $\overline{d_f}$ (resp. $\overline{P_f}$) is the mean fibre diameter (resp. perimeter), $\overline{S_p}$ the mean horizontal section of the pores, ν_c the crucible volume, μ_f the fibre density and m_f the fibre mass in the crucible.

At 898K in dry air at atmospheric pressure, the mean free path value for oxygen is $\overline{\lambda} \approx 0.2$ µm. For the bundle described above, $\overline{d_p}$ lies around 20 µm. Hence, the Knudsen number is low (Kn ~ 0.01); it characterizes bulk diffusion [5]. As the mass Péclet number is very low inside the fibre bundle, mass transfer inside this porous media is restricted to ordinary diffusion of oxygen in air. The vertical diffusion flux per surface unit is given by the formula :

$$j_x(x) = -D\nabla C(x) \tag{6}$$

Integrating the mass balance in the elementary cell (see figure 3) gives the following differential equation for C(x):

$$\frac{d^2C(x)}{dx^2} - \frac{4k_f}{\overline{d_p}D}C(x) = 0 \tag{7}$$

where the boundary conditions are C(x=0)=C_0 and $\frac{dC}{dx}\left(x = L_f\right) = 0$.

After integration, the oxygen concentration inside the porous media is given by :

$$C(x) = C_0 \frac{\cosh\left(\Phi\left(\frac{x}{L_f} - 1\right)\right)}{\cosh\Phi} \tag{8}$$

where $\Phi = L_f/L$ is the Thiele number, with $L = \sqrt{\frac{\overline{d_p}D}{4k_f}}$.

The equality between J_{eff} and the calculated flux at the same abscissa (x=0) leads to :

$$J_{eff} = k_{eff}C_0 = \frac{DC_0}{L}\tanh\Phi \tag{9}$$

The actual oxidation rate of the fibres (k_f) is then an implicit function of k_{eff} :

$$k_{eff} = \frac{D}{L_f}\Phi\tanh\Phi = 2\sqrt{\frac{k_f D}{\overline{d_p}}}\tanh\left(2L_f\sqrt{\frac{k_f}{\overline{d_p}D}}\right) \tag{10}$$

When Φ is lower than 1, mass transfer is limited by heterogeneous reaction and equation (10) becomes:

$$k_{eff} \approx \frac{4L_f}{\overline{d}_p} k_f \qquad (11)$$

k_{eff} and k_f are proportional and as the kinetics law follow Arrhenius relations, the activation energy at the local scale Ea_f (into the fibres bundle) equals the activation energy at the global scale Ea_{eff} : the bundle is considered as an homogeneous reactive surface.

When Φ is higher than 1, diffusional phenomena into the porous material become limiting. Equation (10) approaches the following asymptotic formula:

$$k_{eff} \approx 2\sqrt{\frac{D}{\overline{d}_p}}\sqrt{k_f} \qquad (12)$$

In this case, it follows that $Ea_{eff} = 1/2\ Ea_f$.

3.2. CFD computations

The numerical simulations of gas dynamics flow and reactant species flow in the experimental setup described in part 2.1 are performed with a commercial software [6]. Steady-state solution was attained by a first resolution of the single Navier-Stokes equations, then followed by a coupled resolution of the Navier-Stokes and species balance equations.

Figure 4 shows the geometry of the generated mesh of the cylindrical oxidation reactor. There are 112,200 hexahedral cells and 124,313 nodes in this 3D-geometry.

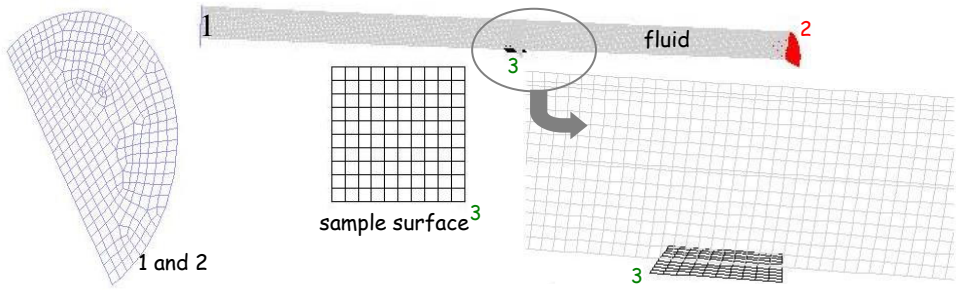

Figure 4: *Mesh of the cylindrical oxidation reactor*

The boundary conditions are:

(1) Inlet: $T = T_0$, mass fraction of air, v = 1 $m.s^{-1}$ (flat velocity profile)

(2) Outlet : P = 101,325 Pa

(3) Wall: heterogeneous reaction (1) (i.e. reactive surface), $k_{eff} = 1e^{-3}$ to $1e^{5}$ $m.s^{-1}$, $T = T_0$

All walls : $T = T_0$

In the following, the reference temperature is given as $T_0 = 898K$.

The transient dynamics flow is solved first and a radial velocity profile above the reactive surface is obtained, as represented on figure 5.

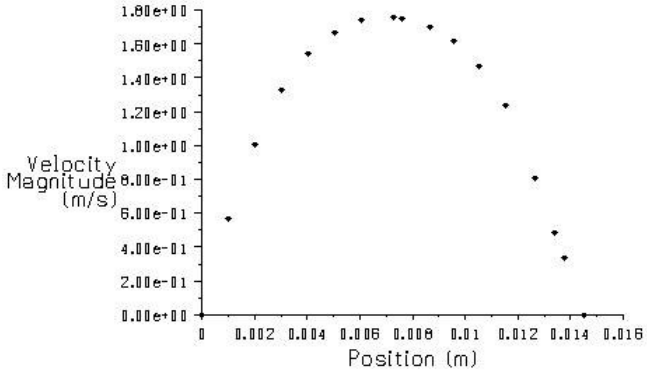

Figure 5: *Radial velocity profile above the reactive surface (v_{entry} = 1 m.s^{-1}, simulation without heterogeneous reaction)*

A parabolic profile is quickly established but velocity increases throughout the tube ; the maximum velocity is at the reactor exit (plane 2). In all parts of the reactor, the mass Péclet number is higher than 1. The oxygen flux brought by convection is therefore sufficient to limit the development of the boundary layer above the reactive surface.

The heterogeneous reaction is then simulated and coupled to the previous numeric result (i.e. the steady-state dynamics flow). No modification of the fluid flow solution is observed.

The oxygen mass fraction on the reactive surface and for different heterogeneous reaction rates give a first indication of the limiting phenomenon (figure 6).

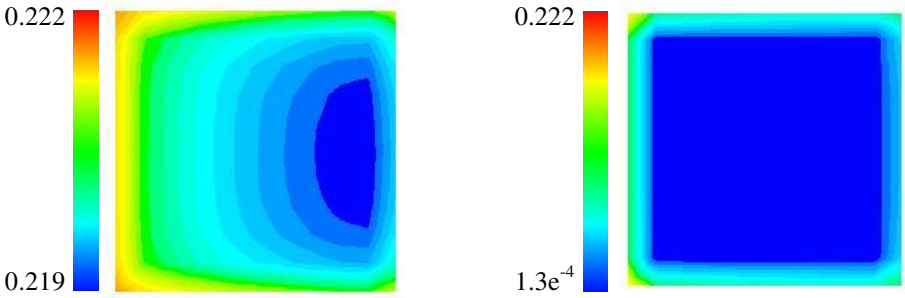

Figure 6: *Mass fraction of oxygen on the reactive surface with (a) k_{eff} = 1e^{-3} m.s^{-1} and (b) k_{eff} = 100 m.s^{-1}*

At low reaction rates (figure 6a), a very small gradient of oxygen concentration is observed. The oxidation is controlled by heterogeneous reaction (reaction-limited regime). At high reaction rates (figure 6b), the gradients of oxygen concentration become important (diffusion-limited regime). For each numerical simulation, the boundary layer thickness is estimated using a plot along an axis normal to the reactive surface (figure

7). We considered the existence of a diffusive boundary layer until the oxygen mass fraction equals 98% of its initial value (i.e. 0.222).

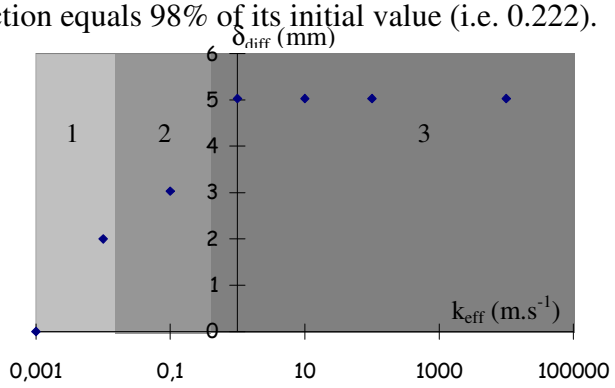

Figure 7*: Boundary layer thickness (δ_{diff}) versus reaction rate (k_{eff}) (1) : reactive regime ; (2) : transient regime ; (3) diffusional regime*

As illustrated by the mass Péclet number study, the boundary layer thickness is never fully developed ; its maximum value does not exceed 35% of the reactor diameter.

The average molar concentration of oxygen on the reactive surface is estimated after surface integration of oxygen molar fraction. The effective mass flow consumption of carbon per unit surface and time is then calculated versus heterogeneous reaction rate (figure 8).

4. IDENTIFICATION

In order to determine the actual oxidation rate of the fibres (k_f), two steps have to be followed:

① and ②: The effective mass flow consumption of the carbon fibres bundle is experimentally assessed. Thus, using figure 8, one can determine the effective reactivity of the carbon fibres bundle k_{eff}.

③ and ④ : The real oxidation rate of the fibres (k_f) is an implicit function of k_{eff} (equation (10) and figure 9). Solving eq. (10) for the estimated value of k_{eff} yields the desired result, that is, k_f.

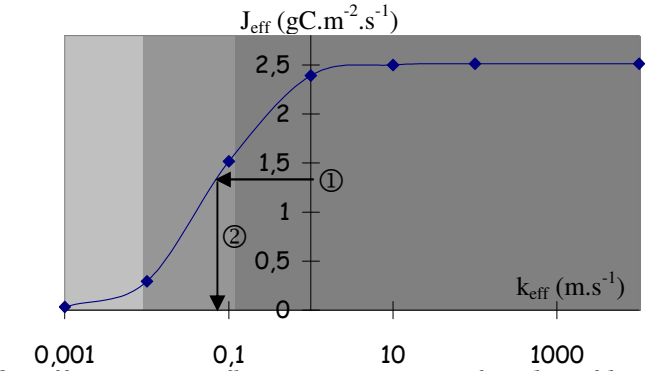

Figure 8: *Effective mass flow consumption of carbon fibres bundle (J_{eff} in g(C).m^{-2}.s^{-1}) versus heterogeneous reaction rate (k_{eff})*

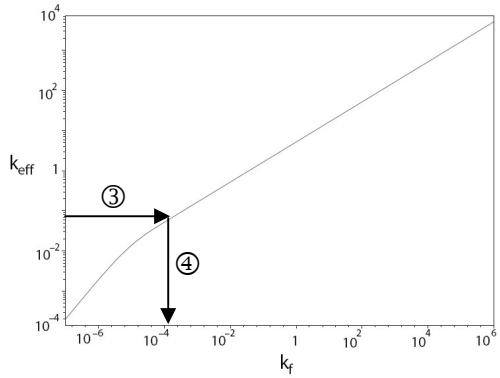

Figure 9: *Plot of k_{eff} ($m.s^{-1}$) versus k_f ($m.s^{-1}$)*

Finally, for reaction-limited and transient regimes, the real oxidation rate of the fibres could be determined from the CFD study and the experimental effective mass flow consumption of carbon fibres bundle. The results are reported in table 2.

Fibre	**Experimental data J_{eff} ($gC/m^2/s$)**	**CFD evaluation k_{eff} ($m.s^{-1}$)**	**Analytical evaluation k_f ($m.s^{-1}$)**
F10	0.04	0.0012	$0.62.10^{-6}$
F5	0.10	0.0026	$0.14.10^{-5}$
F3	0.27	0.0086	$0.54.10^{-5}$
F8	0.30	0.01	$0.65.10^{-5}$
F4	0.41	0.0155	$0.12.10^{-4}$
F6	0.44	0.0168	$0.13.10^{-4}$
F9	0.95	0.042	$0.65.10^{-4}$
F1	1.43	0.082	$0.24.10^{-3}$
F2	2.86	Diffusion-limited regime	Diffusion-limited regime

Table 2: *Experimental mass flow consumption of carbon fibres bundle during oxidation under dry air, at 625°C and 1 atm ; effective reactivity of carbon fibres bundle and real reactivity of carbon fibres*

First, we observed that the oxidation resistance of the raw fibres are in the order : ex-PAN M40, ex-pitch, ex-PAN T300 and ex-cellulose ; this should be expected from the knowledge of their degree of organization. The treatment at 1673K leads to a diminution of the fibres reactivity (reactivity divided by 10 for the ex-PAN M40 fibres and divided by 2 for the ex-pitch fibres). Finally, the graphitization of the ex-PAN T300 fibres leads to a reactivity divided by 10 compared to the reactivity of the same fibres treated only at 1673 K.

The interpretation of the experimental results [2] is now possible by repeating this procedure at all temperature values (*i.e.* numerical simulations, production of plots like figures 8 and 9, and two-step parameter identification).

5. CONCLUSION

In order to obtain a reliable and repeatable experimental method, oxidation tests of carbon materials have been carried out in a cylindrical oxidation reactor at a controlled temperature under dry air at atmospheric pressure. The material tested is a carbon fibres bundle. Modelling transport phenomena in this oxidation reactor has been done using two approaches. First, a dimensionless approach has shown that high Pé and low Da numbers ensure that the oxidation phenomena are globally controlled by reaction mass transfer in the bulk fluid phase. Considering diffusion into the porous bundle, a relation between the effective reaction rate of the fibres bundle (k_{eff}) and the real oxidation rate of the fibres (k_f) has been determined. Then, computational fluid dynamics has been used to simulate the dynamics flow coupled to heterogeneous reaction of carbon with oxygen. The 3D simulations have conduced to the determination of the reactive, transient and diffusional regimes versus effective reaction rate of the fibres bundle. The boundary layer thickness and the effective mass flow consumption of carbon fibres bundle have also been determined. Finally, thanks to the dimensionless approach and the CFD simulations, the experimental data could be expressed in real oxidation rate of the fibres.

REFERENCES

1- **Fitzer, E.** ; "The future of carbon-carbon composites", *Carbon*, **65** (1987) 163.

2- **Avril, L. and Rebillat, F. ;** "Réactivité chimique sous atmosphère oxydante et/ou corrosive de fibres carbone ex-PAN", in *Journées du Groupement Français des Céramiques (GFC)*, mars 2005, Paris, France.

3- **Ong, J.N.** ; "On the kinetics of oxidation of graphite", *Carbon*, **2** (1964) 281-297.

4- **Lachaud, J. ; Aspa, Y. ; Vignoles, G.L. and Goyhénèche, J.M.** ; "Modélisation 3D de l'ablation thermochimique des composites C/C", in *Congrès Français de Thermique*, SFT 2006, Ile de Ré, France, 16-19 May 2006.

5- **Transvalidou, F. and Sotirchos S.V.** ; "Effective diffusion coefficients in square arrays of filament bundles", *AIChE Journal*, **42**, n° 9 (1996) 2426-2438.

6- **Fluent Incorporated**, Fluent 6.1.22, User's guide, 2003